

Lawrence Berkeley National Laboratory

Recent Work

Title

ELECTRONIC STRUCTURE AND OPTICAL PROPERTIES OF Mg_2Si , Mg_2Ge , AND Mg_2Sn

Permalink

<https://escholarship.org/uc/item/7bw863vc>

Authors

Au-Yang, M.Y.

Cohen, M.L.

Publication Date

1969-02-01

UCRL-18788

ey. J

RECEIVED
LAWRENCE
RADIATION LABORATORY

MAR 25 1969

LIBRARY AND
DOCUMENTS SECTION

ELECTRONIC STRUCTURE AND OPTICAL PROPERTIES
OF Mg_2Si , Mg_2Ge , AND Mg_2Sn

M. Y. Au-Yang and M. L. Cohen

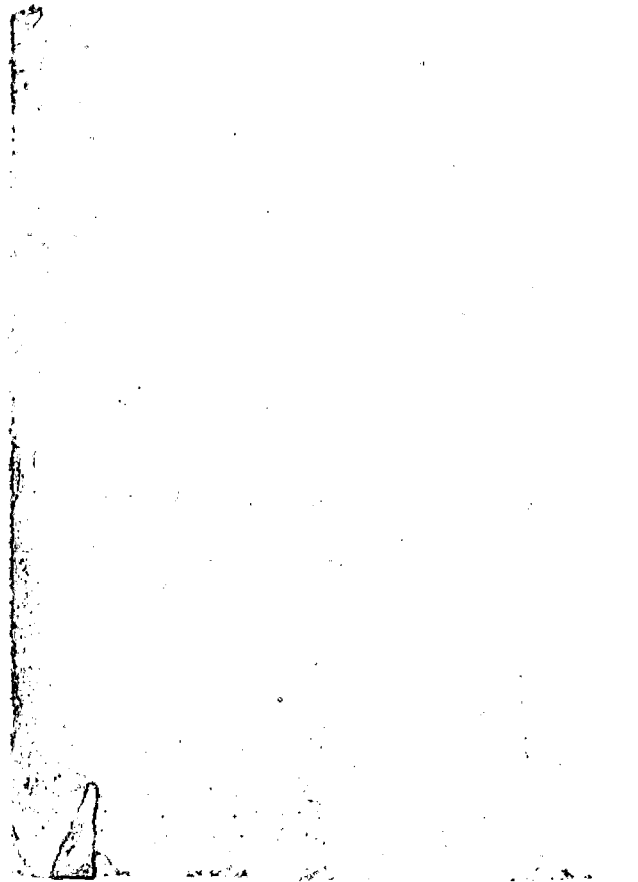
February 1969

TWO-WEEK LOAN COPY

*This is a Library Circulating Copy
which may be borrowed for two weeks.
For a personal retention copy, call
Tech. Info. Division, Ext. 5545*

LAWRENCE RADIATION LABORATORY
UNIVERSITY of CALIFORNIA BERKELEY

UCRL-18788



DISCLAIMER

This document was prepared as an account of work sponsored by the United States Government. While this document is believed to contain correct information, neither the United States Government nor any agency thereof, nor the Regents of the University of California, nor any of their employees, makes any warranty, express or implied, or assumes any legal responsibility for the accuracy, completeness, or usefulness of any information, apparatus, product, or process disclosed, or represents that its use would not infringe privately owned rights. Reference herein to any specific commercial product, process, or service by its trade name, trademark, manufacturer, or otherwise, does not necessarily constitute or imply its endorsement, recommendation, or favoring by the United States Government or any agency thereof, or the Regents of the University of California. The views and opinions of authors expressed herein do not necessarily state or reflect those of the United States Government or any agency thereof or the Regents of the University of California.

Submitted to
Physical Review

UCRL-18788
Preprint

UNIVERSITY OF CALIFORNIA

Lawrence Radiation Laboratory
Berkeley, California

AEC Contract No. W-7405-eng-48

Electronic Structure and Optical Properties
of Mg_2Si , Mg_2Ge , and Mg_2Sn

M. Y. Au-Yang^{melvin} and M. L. Cohen^o

February 1969

R

Electronic Structure and Optical Properties

of Mg_2Si , Mg_2Ge and Mg_2Sn *.

M.Y. Au-Yang

Department of Physics

University of California, Berkeley, California

and

Marvin L. Cohen[†]

Department of Physics and

Inorganic Materials Division,

Lawrence Radiation Laboratory,

University of California, Berkeley, California

Abstract

The electronic band structure and optical constants of Mg_2Si , Mg_2Ge and Mg_2Sn are calculated using the Empirical Pseudopotential Method. The results are compared with experiment.

* Supported in part by the National Science Foundation.

† Alfred P. Sloan Foundation Fellow.

I Introduction

The Empirical Pseudopotential Method¹, EPM, has been used to calculate the band structures and optical constants of many different types of crystals²⁻⁹ with much success. One advantage of using this method is that it yields optical constants which can be directly compared with optical measurements. Recently good reflectance and electroreflectance data on the family of compounds Mg_2Si , Mg_2Ge , and Mg_2Sn were obtained by Scouler¹⁰ and Cardona¹¹. We have, therefore, used the EPM to calculate the band structures and optical constants for these materials in an attempt to understand the optical structure.

Using potentials obtained in previous band structure calculations, we have computed the electronic band structures for Mg_2Si , Mg_2Ge , and Mg_2Sn on a mesh of points in the Brillouin zone. From these points the imaginary part of the dielectric function, $\epsilon_2(\omega)$, is obtained¹², and from $\epsilon_2(\omega)$ the reflection coefficient is calculated. The derivative of the reflection coefficient is also obtained to compare with electroreflectance data.

Lee¹³ and Folland¹⁴ have previously calculated band structures for Mg_2Si , and Lee also gave the results for Mg_2Ge ; however, neither calculation gives optical constants for these compounds, and the two results for Mg_2Si do not agree with each other. We have compared our results with these calculations and we have used a critical point analysis of the interband energy contours to identify the structure in the $\epsilon_2(\omega)$ curves in terms of interband transitions. Our analysis shows that the previously existing calculations cannot yield optical constants that are consistent with experiment to within one eV. Our results, however, agree very well with experiment; the discrepancy between theory and experiment over the entire region of interest (0 to 10 eV) is within .4eV for all three compounds.

We also found that the peak heights in our calculated optical spectrum agree well with experiment. The agreement is better than that obtained in more ionic crystals²⁻⁷. We believe that this agreement results from the lack of exciton like binding between the electron hole pair because of the large static dielectric constants of these crystals.

This paper will be divided into three sections. Section II discusses the pseudopotential Hamiltonian and the form factors. In Section III, the results are given and comparison with experiment is made in the following order: reflectance, electro-reflectance and energy gap measurements. Section III concludes with a comparison of our results with those of Lee and Folland.

II. Calculations

The EPM involves the variation of pseudopotential form factors to fit optical data¹. In this work, we imposed two further restrictions: the form factors were chosen to yield close agreement not only with optical data, but also with existing form factors for the individual constituent elements, the group IV elements^{1,14} and Mg¹⁵. Furthermore, the same pseudopotential was used for the Mg ion in the three compounds. The success of the calculations indicates the correctness of associating a pseudopotential with an ion, independent of its chemical state. Screening effects should modify the pseudopotential, but the differences are expected to be small for similar non-metallic compounds.

To calculate the band structure, we assume an energy independent pseudopotential, so that the pseudo-Hamiltonian is:

$$H = - \left(\frac{\hbar^2}{2m} \right) \nabla^2 + V(\underline{r}) . \quad (1)$$

The weak pseudopotential is expanded in the reciprocal lattice

$$V(\underline{r}) = \sum_{\underline{G}} V(\underline{G}) e^{-i\underline{G} \cdot \underline{r}} \quad (2)$$

where \underline{G} is a reciprocal lattice vector. For the compounds Mg_2X , where X is Si, Ge and Sn, the structure is cubic fluorite. The lattice is FCC with three atoms per primitive cell. The element X occupies a lattice site, and the magnesium atoms are at $\pm \underline{u}$, where $\underline{u} = (\frac{1}{4}, \frac{1}{4}, \frac{1}{4})a$, and a is the length of the cube. Thus we can write

$$\begin{aligned}
 V(\underline{Q}) &= \frac{1}{\Omega_{\text{cell}}} \int_{\text{cell}} V(\underline{r}) e^{i\underline{Q} \cdot \underline{r}} d^3\underline{r} \\
 &= \frac{1}{\Omega_{\text{cell}}} \left[\int_{\text{X}} V^{\text{X}}(\underline{r}) e^{i\underline{Q} \cdot \underline{r}} d^3\underline{r} \right. \\
 &\quad \left. + \sum_{p=\pm 1} e^{i p \underline{u} \cdot \underline{Q}} \int_{\text{Mg}} V^{\text{Mg}}(\underline{r}) e^{i\underline{Q} \cdot \underline{r}} d^3\underline{r} \right] \quad (3)
 \end{aligned}$$

where Ω_{cell} is the volume of the primitive cell. Writing $\underline{Q} = (h, k, \ell) \frac{2\pi}{a}$, we have

$$V(\underline{Q}) = \frac{1}{\Omega_{\text{cell}}} \left[\Omega_{\text{X}} V^{\text{X}}(\underline{Q}) + 2\Omega_{\text{Mg}} V^{\text{Mg}}(\underline{Q}) \cos\left\{\frac{\pi}{2}(h+k+\ell)\right\} \right] \quad (4)$$

where Ω_{X} and Ω_{Mg} are the volume per atom of X and Mg respectively; $V^{\text{X}}(\underline{Q})$ and $V^{\text{Mg}}(\underline{Q})$ are the corresponding pseudopotentials. We will assume spherically symmetric atomic pseudopotentials and thus $V(\underline{Q}) = V(|\underline{Q}|)$.

Taking the pseudopotentials of Si, Ge and Sn from Cohen and Bergstresser¹ (CB) and that of Mg from Animalu and Heine¹⁵, we find non-vanishing form factors only for $|\underline{Q}|^2 \leq 20 \left(\frac{2\pi}{a}\right)^2$. For the FCC lattice, there are 8 such form factors. Using Eq. (4) we can write these form factors in terms of the atomic form factors, as shown in the third column of Table I. We note that because the lattice constants of Mg_2X are different than the lattice constants of the elements, the values of the atomic pseudopotentials are obtained by interpolation from a smooth curve drawn from the known atomic pseudopotential form factors.

To calculate the optical properties from the band structure, we first calculate $\epsilon_2(\omega)$. To do this we use the expression

$$\epsilon_2(\omega) = \frac{e^2 \hbar^2}{3\pi m^2 \omega^2} \sum_{c,v} \int \delta(E_c(\mathbf{k}) - E_v(\mathbf{k}) - \hbar\omega) |\langle U_{\mathbf{k},v} | \nabla | U_{\mathbf{k},c} \rangle|^2 d^3 \mathbf{k} \quad (5)$$

where c, v stands for conduction and valence bands, and $U_{\mathbf{k},n}$ is the periodic part of the n^{th} band wavefunction. We approximate the exact $U_{\mathbf{k},n}$ by the eigenfunction of the pseudo-Hamiltonian, Eq. (1). The numerical evaluation of this expression for the FCC lattice is discussed elsewhere³.

The function $\epsilon_1(\omega)$ is obtained from $\epsilon_2(\omega)$ by using the Kramers-Kronig relations with an approximate tail function for $\omega > \omega_c$, where ω_c is the largest ω for which $\epsilon_2(\omega)$ is calculated. The reflection coefficient is obtained from $\epsilon_1(\omega)$, $\epsilon_2(\omega)$.

III Results

The band structures obtained using the form factors in Table I for Mg_2Si , Mg_2Ge and Mg_2Sn are shown in Fig. 1, 2, and 3 for symmetry directions of the Brillouin Zone. In Figs. 4, 5 and 6 we plot the calculated and experimental $\epsilon_2(\omega)$ for the three compounds. The experimental $\epsilon_2(\omega)$ was obtained from reflectivity data by Kramers-Kronig transformation. In Fig. 7 we plot the pseudopotential form factors used in the calculations for the Group IV elements and magnesium. For the Group IV elements we compare the form factors with those of Cohen and Bergstresser (CB). We see that for Si and Ge, a smooth curve can be drawn through the pseudopotential form factors used here and those of CB. However, for Sn, we were forced to change the pseudopotential of CB slightly. The differences in energy of .02 Rydberg, however, is smaller than the spin-orbit coupling energy for Sn which we neglected. For magnesium, we compared our potential with the potential calculated by Animalu and Heine¹⁵ and that used by Kimball, Stark and Mueller¹⁶.

Inspection of Figs. 1 through 6 illustrates that the band structures and the $\epsilon_2(\omega)$ curves for the three compounds are similar. We shall first discuss their common features, and then discuss these band structures individually by comparison with reflectivity data (Section IIIb), electro-reflectance data (Section IIIc), energy gap measurements (Section IIId) and the existing band structure calculations of Lee and Folland (Section IIIe).

IIIa Common Features

The valence band maximum is at Γ , with symmetry Γ_{15} , and the conduction band minimum is at X. The fundamental energy gap is thus indirect. The symmetry of the conduction band minimum is either X_1 or X_3 , but these two levels are close together. These features best exhibit themselves in electrical measurements.

The optical structure of these compounds can best be identified by a critical point analysis. If one examines carefully the band structure and its associated $\epsilon_2(\omega)$ curve, it is possible to identify the interband transitions between valence and conduction states contributing to $\epsilon_2(\omega)$: the important transitions come from pairs of bands for which the joint density of states is near a singularity. The singular points of the zone are called critical points (cp's), and they give rise to structure in $\epsilon_2(\omega)$. An analysis of these critical points explains the general similarities of the $\epsilon_2(\omega)$ curves for the three compounds. For example, we find that the 4th and 5th bands along Σ , the 4th and 6th bands along Δ , and the 4th, 5th and 6th bands along Λ are almost parallel over a large region of the zone for all the three compounds and thus the joint density of states is large there. Furthermore, the X_{1-5} gap is at about the same energy as the Σ_{4-5} cp. The main peak, which results mainly from the Σ_{4-5} transitions, thus has a large magnitude. Another important fact to notice is that the energy separation of the 4th and 5th bands along Λ is always below the main peak, whereas that of the 4th and 6th bands along Λ is always above. These three main contributions to $\epsilon_2(\omega)$ therefore dictate the general three-peak shape of the $\epsilon_2(\omega)$ curve (though the first peak merges with the main peak in Mg_2Si and Mg_2Sn).

Now we shall discuss the optical structure of each compound separately.

IIIb Reflectance

Mg₂Si (Figs. 1 and 4)

The experimental $\epsilon_2(\omega)$ curve starts with an indirect tail at about .6eV. These indirect transition contributions are not included in the calculations, however: the theoretical $\epsilon_2(\omega)$ curve starts at 2.1eV resulting from the $\Gamma_{15} \rightarrow \Gamma_1$ transition with an associated cp of M_0 symmetry. This structure can be identified with the sharp rise at about 2eV in the experimental $\epsilon_2(\omega)$.

The following is a discussion of the major contributions to the theoretical $\epsilon_2(\omega)$; a comparison of the critical points in the experimental and theoretical $\epsilon_2(\omega)$ curves as a function of energy for all three compounds is given in Table II.

Above the threshold for the direct transition there is the 2.2eV $L_3' \rightarrow L_1$ transition which is closely followed by the 2.4eV $\Lambda_3 \rightarrow \Lambda_1$ transition. The associated cp's have M_0 and M_3 symmetry respectively. The main peak starts at about 2.6eV; the transitions responsible are $X_5' \rightarrow X_1$, $X_5' \rightarrow X_3$, and $K_4 \rightarrow K_1$, all having M_0 symmetry. As stated earlier, the large region of the zone along Δ , the $\Lambda_5 \rightarrow \Delta_2'$ transitions, gives a large contribution above the $X_5' \rightarrow X_3$ gap of 2.6eV. The peak structure of the main peak is a result of M_2 and M_3 cp's arising from $\Sigma_4 \rightarrow \Sigma_1$ and $\Delta_5 \rightarrow \Delta_2'$ transitions respectively at about 3.0eV.

Above the main peak the next structure is a peak at 3.7eV which arises from $L_3' \rightarrow L_3$, and $\Lambda_3 - \Lambda_3$ transitions of types M_2, M_3 ; $\Delta_5 - \Delta_1$ transitions also contribute an M_3 in this region. Above this peak there are a large number of different regions in the zone contributing to $\epsilon_2(\omega)$. We can associate part of the contributions from 4.5eV to 5eV to the $\Delta_1 \rightarrow \Delta_1$, $K_1 \rightarrow K_1$, $K_3 \rightarrow K_1$ and

$X_4' \rightarrow X_1$ transitions (see Table II). These contributions give rise to a bump at around 5 eV.

Inspection of Table II and Fig. 4 shows that there is good agreement between theory and experiment both for the magnitudes and positions in energy of the structure in $\epsilon_2(\omega)$. Even the last bump at 5 eV shows up well in the experimental curve.

Mg₂Ge (Figs. 2 and 5)

For Mg₂Ge the experimental indirect tail starts at .7eV which compares fairly well with our calculated value for the indirect gap of .92eV. The theoretical threshold arises from the $\Gamma_{15} \rightarrow \Gamma_1$ transition at 1.5eV with a cp of type M₀. At higher energies the M₀ and M₃ cp's arising from $L_3' \rightarrow L_1$ (2.0eV) and the $\Lambda_3 \rightarrow \Lambda_1$ (2.2eV) transitions contribute as in Mg₂Si. The main peak, however, does not start until about 2.9eV where we have an M₀ cp coming from $X_5' \rightarrow X_3$ transitions. The large separation in energy between the "LA" contributions and the start of the main peak results in a "LA" peak (Fig. 5) instead of a "LA" shoulder (Fig. 4) as in the Mg₂Si case. The $\Delta_5 \rightarrow \Delta_2'$ transitions again contribute, but not as much as in the Mg₂Si case because these bands do not give a cp. The peak structure arises partially from M₀ cp's of the $K_4 \rightarrow K_1$ and $X_5' \rightarrow X_1$ transitions at 3.0eV, and the main contribution comes from the M₂ cp of the $\Sigma_4 \rightarrow \Sigma_1$ transition. The M₃ cp of the $\Gamma_{15} \rightarrow \Gamma_{25}'$ transition is at 3.2eV. The last peak, from 3.9 to 4.2 eV is again the result of $\Delta_5 \rightarrow \Delta_1$ (M₃), $L_3' \rightarrow L_3$ (M₂) and $\Lambda_3 \rightarrow \Lambda_3$ (M₃) transitions. Finally, we again have a group of cp contributions creating a bump at 5.2eV.

The comparison between theory and experiment can now be made by looking at Table II and Fig. 5. There is good agreement between the curves for the positions in energy of the structure in $\epsilon_2(\omega)$.

However, the magnitude of the first "LA" peak is appreciably bigger on the experimental curve. Although part of this discrepancy may have been the result of using pseudo-matrix elements in the calculation of $\epsilon_2(\omega)$, the large experimental peak may have been caused by the tail function used in the Kramers Kronig transform of the reflectivity¹⁰. Finally as for Mg_2Si , we again see the bump at 5.2 in the experimental $\epsilon_2(\omega)$.

Mg_2Sn (Figs. 3 and 6)

The experimental tail starts at a low value of .2eV which does not compare too favorably with our value of .64eV for the indirect gap. However, the data was taken at 77°K, and at this temperature the fundamental gap should be almost .03eV below its value at 0°K¹⁷. The discrepancy is therefore only about .4eV.

The threshold for the direct transitions again arises from $\Gamma_{15} \rightarrow \Gamma_1$ transitions. The cp is of type M_0 and its energy value is 1.1eV. Above this energy we have the usual "LA" contributions at 2.0eV which come from the M_0 and M_3 cp's from the $L_3' \rightarrow L_1$ and $\Lambda_3 \rightarrow \Lambda_1$ transitions respectively. The $X_5' \rightarrow X_1$ and $K_4 \rightarrow K_1$ cp's, which in both the Mg_2Si and Mg_2Ge cases are coincident with either the $X_5' \rightarrow X_3$ or the main peak, are here distinct. These M_0 cp's are at 2.4 and 2.7eV respectively, thus creating two extra bumps on the low energy side of the main peak. It is unfortunate that these fine points in the structure are smoothed out in the $\epsilon_2(\omega)$ plot and cannot be seen.

The main peak structure itself comes from $\Sigma_4 \rightarrow \Sigma_1$ transitions with an M_2 cp at 2.8eV. The $\Delta_5 \rightarrow \Delta_2'$ transitions, as in the Mg_2Ge case, do not have a cp, and so the magnitude of the main peak is of the same size as that of Mg_2Ge and is appreciably smaller than that of Mg_2Si . The $\Delta_5 \rightarrow \Delta_2'$

transitions contribute mostly near Γ and X; the M_0 of $\Gamma_{15} \rightarrow \Gamma_{25}'$ at 2.9eV and the M_1 of $X_5' \rightarrow X_3$ at 3eV contribute to the main peak.

The last important peak is again a "LA" peak, except here the $\Delta_5 \rightarrow \Delta_1$ contribution has moved down to the main peak, and so only $L_3' \rightarrow L_3$ ($M_2, 3.5\text{eV}$) and $\Lambda_3 \rightarrow \Lambda_3$ ($M_3, 3.7\text{eV}$) contribute. Above this peak we again have a group of cp contributions from about 4.2 to 4.6eV creating a bump at about 4.4eV.

A comparison of theory and experiment (Fig. 6 and Table II) shows good agreement in the positions of the principal structure in the $\epsilon_2(\omega)$. The larger magnitude of the experimental $\epsilon_2(\omega)$ on the low energy side of the main peak can be attributed to the indirect transitions which we have neglected. They are more important here than in the previous cases because the indirect gap is much smaller here. Finally, we again find the bump (at 3.9eV) above the last "LA" peak in the experimental $\epsilon_2(\omega)$; however in this case the agreement in energy between theory and experiment is not as good as in the previous cases. One factor which may be responsible for this discrepancy is our neglect of the spin-orbit coupling, which is larger for Sn than for either Ge or Si.

IIIc Electro-Reflectance

While it is generally possible to see most of the critical points in the $\epsilon_2(\omega)$ curve, the cp's show up much clearer in the first derivative of $\epsilon_2(\omega)$. The reason is that the slope of $\epsilon_2(\omega)$ at a cp is infinite. This derivative technique is used experimentally in electro-reflectance measurements.

For the M_2X compounds, Cardona¹¹ has made electro-reflectance measurements in the 1.5eV to 4.5eV range. We can make an approximate comparison between Cardona's data with our calculations by identifying the correspondence between the structure in the $\Delta R/R$ curve in the electro-reflectance measurements with $(\frac{dR}{d\omega})/R$ of our calculations. In Table III we tabulate the results. The agree-

ment is seen to be good. Some of the structure missing in the $\epsilon_2(\omega)$ can easily be identified.

IIIId Energy Gap Measurements

The fundamental gaps for these three compounds has been measured electrically and optically¹⁷⁻²². In Table IV we compare our results with experiment. The agreement is within .4eV. We remark that for Mg_2Si we can raise the calculated gap to agree with experiment if we raise the energy of the main peak also. For Mg_2Ge and Mg_2Sn we notice that the gaps are both bigger than the experimental values, but since the spin-orbit interaction lowers these gaps, the agreement with experiment will be better if spin-orbit effects are included. The calculations show that the fundamental gaps are indirect; for Mg_2Si and Mg_2Ge , this appeared to be consistent with experiment²³.

IIIe Comparison With Existing Calculations

If we compare our results with the two existing calculations for Mg_2Si , we find that our results are radically different from Folland's;¹⁴ however, we find that Lee's¹³ results are similar to ours with some shifts in the energies. The energy differences can be traced in part to the magnesium potential which was used in the two calculations. If we look at Fig. 7 and Table I, we see that there is considerable contribution from the magnesium potential for $|k| > 2k_F$. However, in Lee's calculations an exponential tail function which vanishes at about $|k| = 2.4$ atomic units for $|k| > 2k_F$ was used. Thus Lee's effective pseudopotential (i.e. $V(|G|)$ on Table I) is bigger on the average, resulting in bigger energy differences. We would, therefore, expect an $\epsilon_2(\omega)$ curve derived from Lee's band to be similar to ours in shape, but the main structure would have higher energies compared with our result. Inspection

shows that the shift in energy is about 1eV.

In conclusion, we would say that our calculations quite successfully explain the data on Mg_2Si , Mg_2Ge and Mg_2Sn . The band structures were calculated to fit optical structure using potentials which are consistent with those used in existing calculations for other crystals. We note that the minor structure in the measured optical spectra are also reproduced in the calculations.

Acknowledgements

We would like to thank Dr. W.J. Scouler for allowing us to use his results prior to publication and to Dr. Samuel Bowen for many helpful discussions.

This work was done under the auspice of the United States Atomic Energy Commission through the Inorganic Materials Research Division of the Lawrence Radiation Laboratory.

1. M.L. Cohen and T.K. Bergstresser, Phys. Rev. 141, 789 (1966) and references therein.
2. C. Fong, W. Saslow and M.L. Cohen, Phys. Rev. 168, 992 (1968).
3. W. Saslow, T.K. Bergstresser, C.Y. Fong and M.L. Cohen, Solid State Comm. 5, 667 (1967).
4. M.L. Cohen, Proceedings of the International Conference on II-VI Semiconducting Compounds, (W.A. Benjamin, Inc., New York, 1967), p. 462.
5. T.K. Bergstresser and M.L. Cohen, Phys. Rev. 164, 1069 (1967).
6. P.J. Lin, W. Saslow, and M.L. Cohen, Solid State Comm. 5, 893 (1967).
7. C.Y. Fong and M.L. Cohen, to be published.
8. D. Brust, J.C. Phillips and F. Bassani, Phys. Rev. Letters 2, 94 (1962).
9. D. Brust, M.L. Cohen and J.C. Phillips, Phys. Rev. Letters 2, 339 (1962).
10. W.J. Scouler, to be published.
11. M. Cardona, to be published.
12. D. Brust, Phys. Rev. 134, A1337 (1964).
13. P.M. Lee, Phys. Rev. 135, A1110 (1964).
14. N.O. Folland, Phys. Rev. 158, 764 (1968).
15. A.O.E. Animalu and V. Heine, Phil. Mag. 12, 1249 (1965).
16. J.C. Kimball, R.W. Stark and P.M. Mueller, Phys. Rev. 162, 600 (1967).
17. U. Winkler, Helv. Phys. Acta 28, 633 (1955).
18. R.G. Morris, R.D. Redin and G.C. Danielson, Phys. Rev. 109, 1909 (1958).
19. R.D. Redin, R.G. Morris and G.C. Danielson, Phys. Rev. 109, 1916 (1958).
20. R.F. Blunt, H.P.R. Frederikse and W.R. Hosler, Phys. Rev. 100, 663 (1955).
21. M.W. Heller and G.C. Danielson, J. Phys. Chem. Solids 23, 601 (1962).
22. A. Stella and D.W. Lynch, J. Phys. Chem. Solids 25, 1253 (1964).
23. P.H. Koenig, D.W. Lynch and G.C. Danielson, J. Phys. Chem. Solids 20, 122 (1961).

- I. The pseudopotential form factors for Mg_2X ;

$$V_1 = \frac{\Omega_X}{\Omega_{\text{cell}}} V^X(|G|); \quad V_2 = \frac{2\Omega_{Mg}}{\Omega_{\text{cell}}} V^{Mg}(|G|)$$

and G is in units of $\frac{2\pi}{a}$, where a is the side of the cube for the Mg_2X lattice.

- II. The calculated transition energies for Mg_2Si , Mg_2Ge and Mg_2Sn and their identifications. The experimental transition energies, when identified, are shown in parenthesis.
- III. The electroreflectance structure and its comparison with theory between 1.5 and 4.5 eV. The identifications are also given. Some structure is found both in the theoretical and experimental curves; however, these do not appear to be associated with a single critical point.
- IV. The calculated and experimental fundamental energy gaps for Mg_2Si , Mg_2Ge and Mg_2Sn . Unless otherwise specified, these values are given for $0^\circ K$.

Table I

Pseudopotential Form Factors, in Ryd.

g	$ g^2 $	$v(g)$	Mg_2Si		Mg_2Ge		Mg_2Sn	
			V^{Mg}	V^{Si}	V^{Mg}	V^{Ge}	V^{Mg}	V^{Sn}
(111)	3	V_1	--	-.33	----	-.34	----	-.23
(200)	4	$V_1 - V_2$	-.03	-.215	-.03	-.203	-.045	-.215
(220)	8	$V_1 + V_2$.06	-.015	.06	-.043	.07	-.01
(311)	11	V_1	----	.039	----	.035	----	.02
(222)	12	$V_1 - V_2$.04	.055	.04	.05	.049	.02
(400)	16	$V_1 + V_2$.025	.079	.025	.052	.035	.006
(331)	19	V_1	----	.056	----	.01	----	0.
(420)	20	$V_1 - V_2$.01	.04	.01	0.	.015	0.

Table II

Transition	Type of Singularity			Energy in eV		
	Mg ₂ Si	Mg ₂ Ge	Mg ₂ Sn	Mg ₂ Si	Mg ₂ Ge	Mg ₂ Sn
$\Gamma_{15} \rightarrow \Gamma_1$	M ₀	M ₀	M ₀	2.06 (2.1)	1.49 (1.6)	1.06
$L_{3'} \rightarrow L_1$	M ₀	M ₀	M ₀	2.15	1.99 (2.1)	1.97
$\Lambda_3 \rightarrow \Lambda_1$	M ₃	M ₃	M ₃	2.39	2.22	2.03
$X_{5'} \rightarrow X_1$	M ₀	M ₀	M ₀	2.62 (2.5)	3.01	2.35 (2.3)
$\Delta_5 \rightarrow \Delta_{2'}$	M ₃	no cp	no cp	2.81	----	----
$X_{5'} \rightarrow X_3$	M ₀	M ₀	M ₁	2.74	2.84	3.02
$(K_4 \rightarrow K_1)_{45}$	M ₀	M ₀	M ₀	2.74	3.03	2.69 (2.5)
$\Gamma_{15} \rightarrow \Gamma_{25'}$	M ₀	M ₃ or M ₀	M ₀	2.80	3.20	2.94
$\Sigma_4 \rightarrow \Sigma_1$	M ₂	M ₂	M ₂	3.01 (2.7)	3.16 (3.0)	2.83 (2.7)
$L_{3'} \rightarrow L_3$	M ₂	M ₂	M ₂	3.59 (3.7)	4.08 (4.1)	3.52 (3.4)
$\Lambda_3 \rightarrow \Lambda_3$	M ₃	M ₃	M ₃	3.79	4.22	3.71
$\Delta_5 \rightarrow \Delta_1$	M ₃	M ₃	M ₃	3.87	3.94	3.24
$(K_1 \rightarrow K_1)_{23}$	M ₀	M ₀	M ₀	4.59	4.74	4.16
$\Delta_1 \rightarrow \Delta_1$	M ₀	no cp	M ₀	4.60	----	4.23
$\Delta_1 \rightarrow \Delta_1$	M ₁	no cp	M ₁	4.63	----	4.29
$X_{4'} \rightarrow X_1$	M ₁	M ₁	M ₁	5.03	5.37	4.27
$(K_3 \rightarrow K_1)_{35}$	M ₀	M ₀	M ₀	5.06	5.29	4.55

Energy of Structure (eV)

Transition	Mg ₂ Si		Mg ₂ Ge		Mg ₂ Sn	
	Theory	Exp.	Theory	Exp.	Theory	Exp.
$\Gamma_{15} \rightarrow \Gamma_1$	2.05	2.27	1.7	1.64	1.3	---
$\Lambda_3 \rightarrow \Lambda_1$	2.4	2.51	2.3	2.37	2.1	1.96
$X_5' \rightarrow X_1$	---	---	---	---	2.35	2.24
$K_4 \rightarrow K_1$	2.9	2.78	3.1	2.71	2.8	2.48
$\Sigma_4 \rightarrow \Sigma_1$	3.18	3.05	3.3	2.88	3.1	2.70
-----	3.4	3.28	3.7	3.31	3.25	2.96
$\Lambda_3 \rightarrow \Lambda_3$	3.7	3.8	4.1	4.03	3.60	3.60
-----	---	---	---	---	3.8	3.86

Table IV

	<u>Calculated Indirect Gap</u>	<u>Experimental Gap</u>	<u>Reference</u>
Mg ₂ Si	.53	.78	18
		.80	21
		.77	17
		.69*	22
Mg ₂ Ge	.92	.65	10
		.69	19
		.74	17
		.67*	22
Mg ₂ Sn	.64	.76	10
		.33	20
		.36	17
		.23	10

* at 15° K.

1. The band structure of Mg_2Si .
2. The band structure of Mg_2Ge .
3. The band structure of Mg_2Sn .
4. The calculated and experimental imaginary part of the dielectric function, $\epsilon_2(\omega)$, for Mg_2Si .
5. The calculated and experimental imaginary part of the dielectric function, $\epsilon_2(\omega)$, for Mg_2Ge .
6. The calculated and experimental imaginary part of the dielectric function, $\epsilon_2(\omega)$, for Mg_2Sn .
7. The pseudopotentials of the elements Si, Ge, Sn, and Mg; a is the lattice constant for the semiconductor element and k_F is the Mg Fermi momentum. The open circles are the form factors used in the calculations. For Si, Ge, and Sn the closed circles are the form factors of CB. For Mg, the closed circles are the form factors of Kimball, Stark, and Mueller; the smooth curve is that of Animalu and Heine.

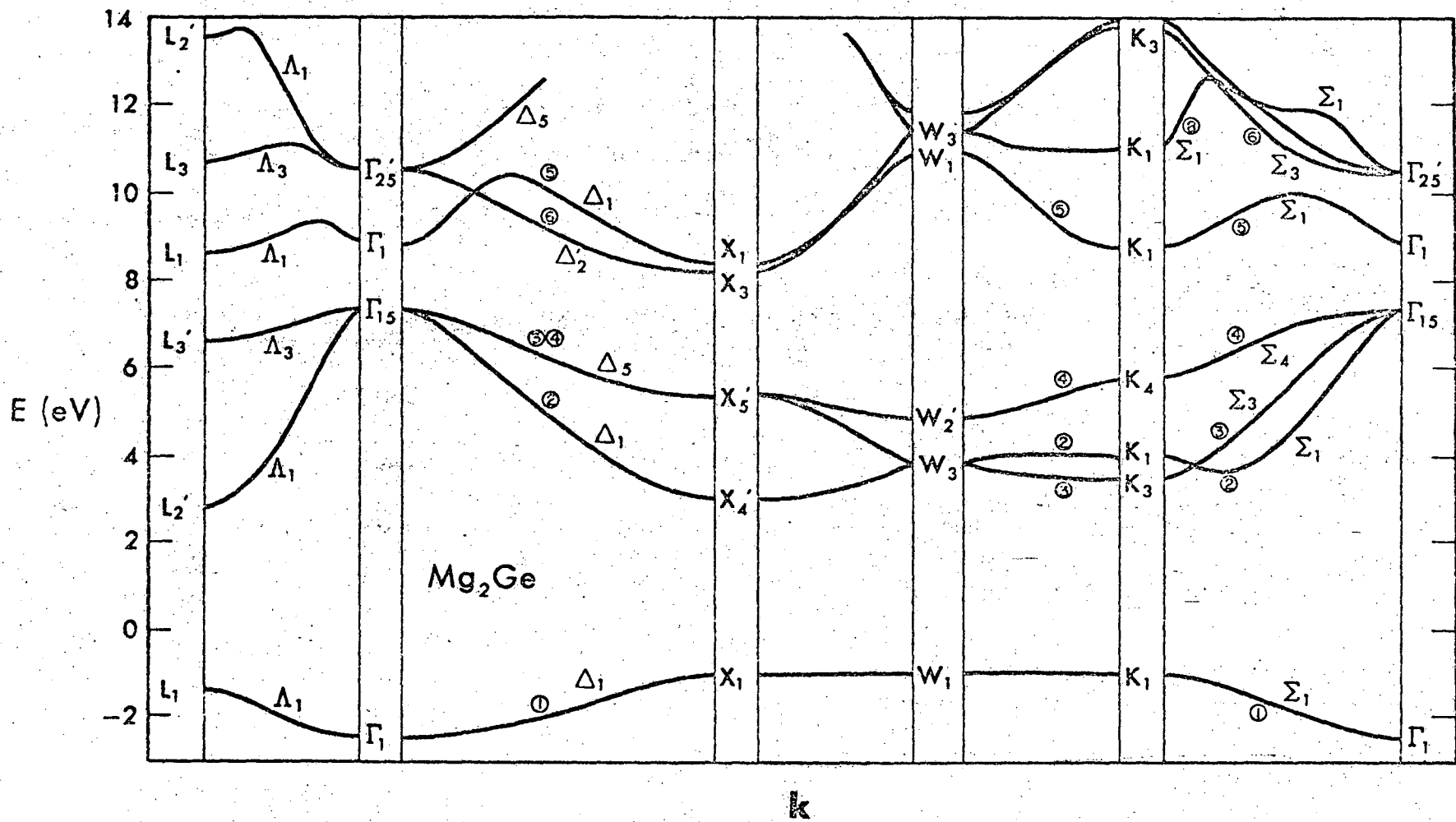


Fig. 2

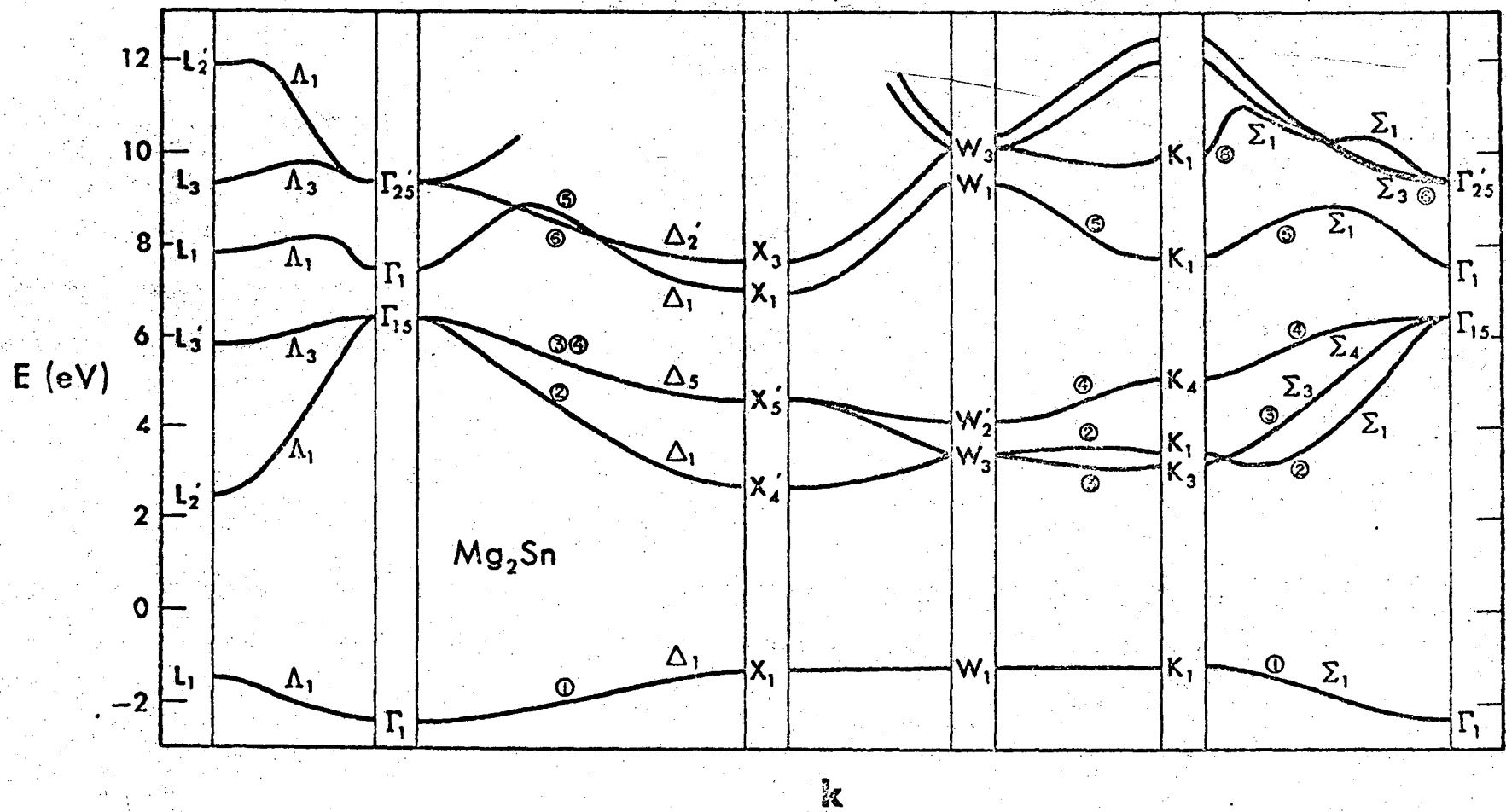


Fig. 3

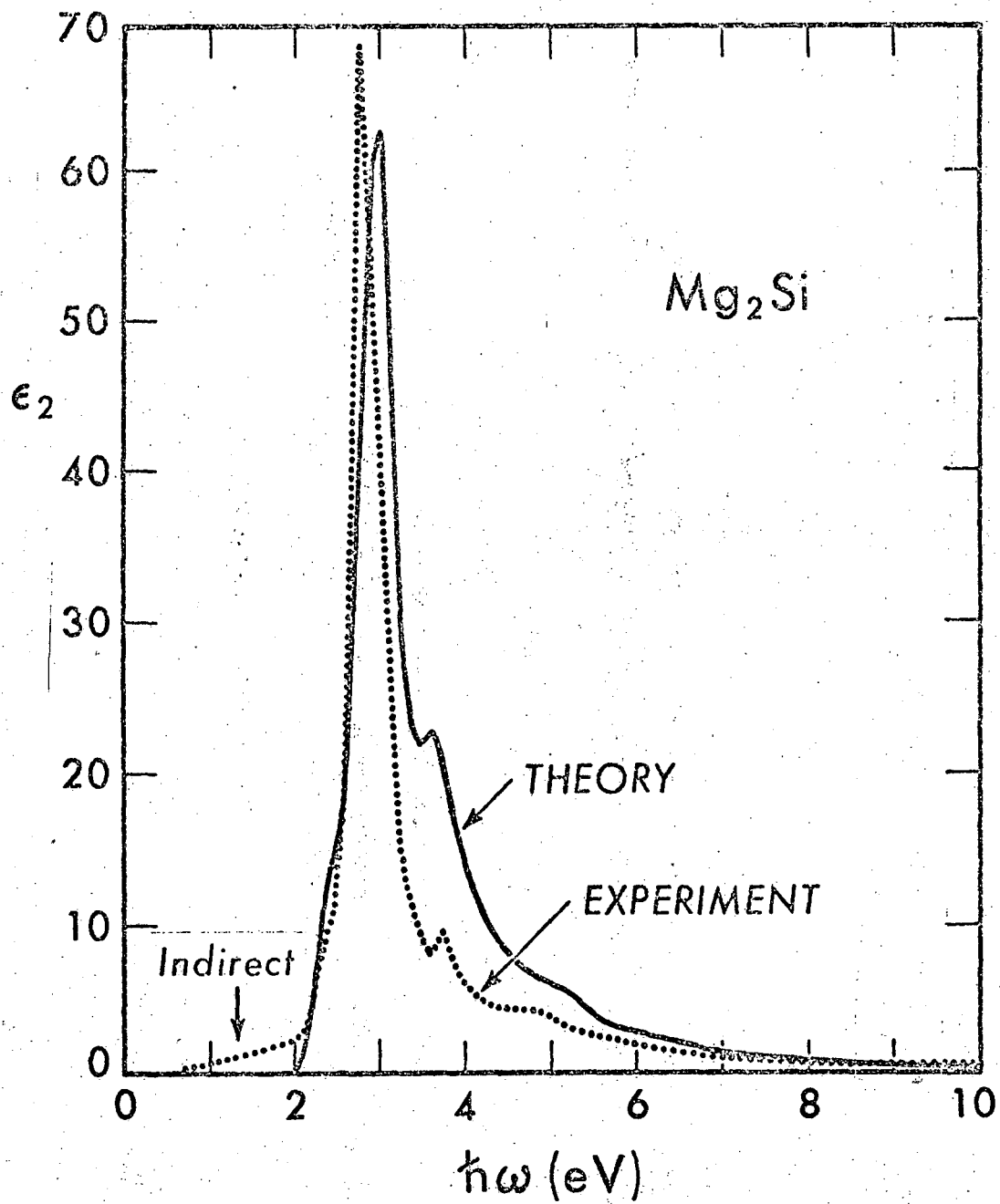


Fig. 4

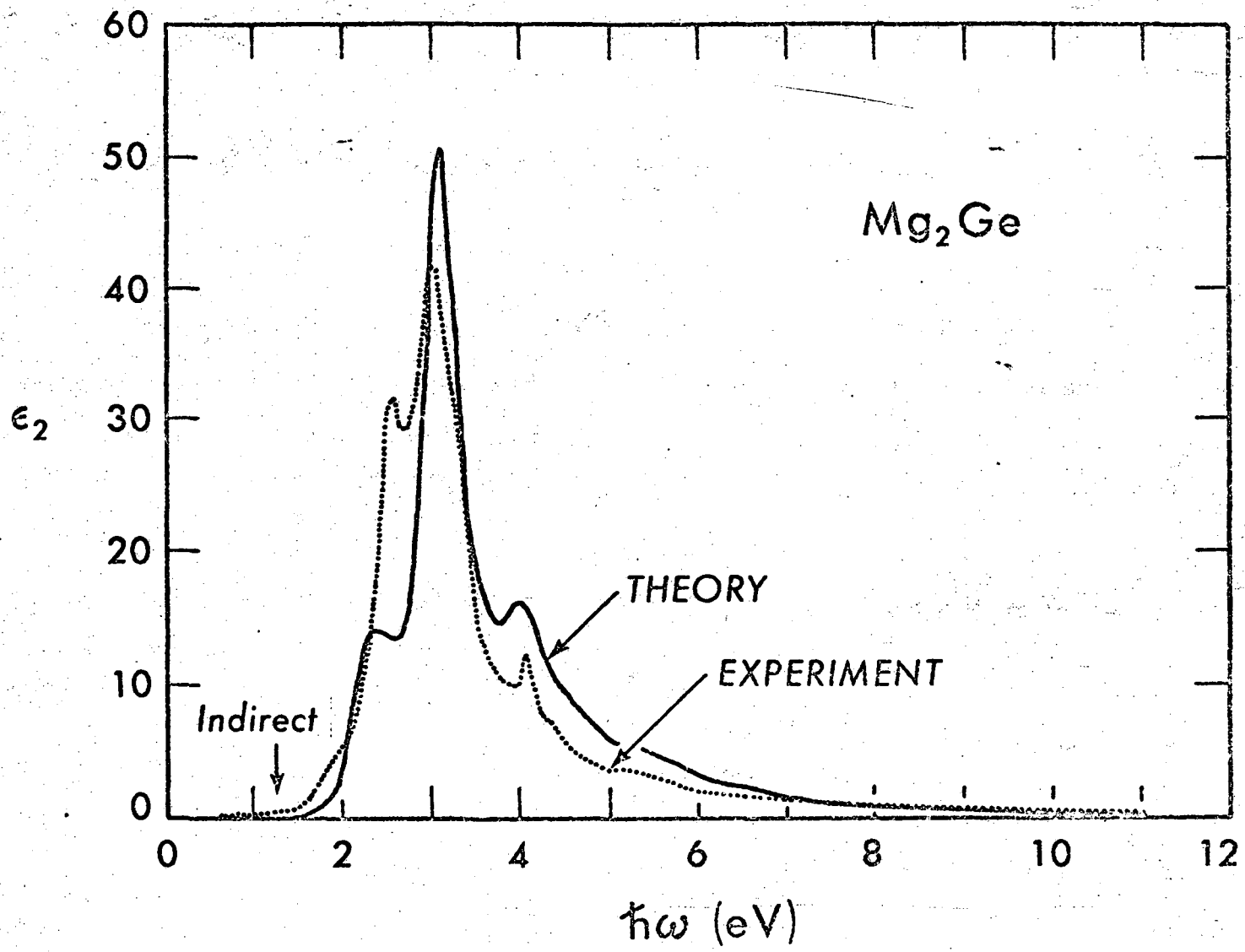


Fig. 5

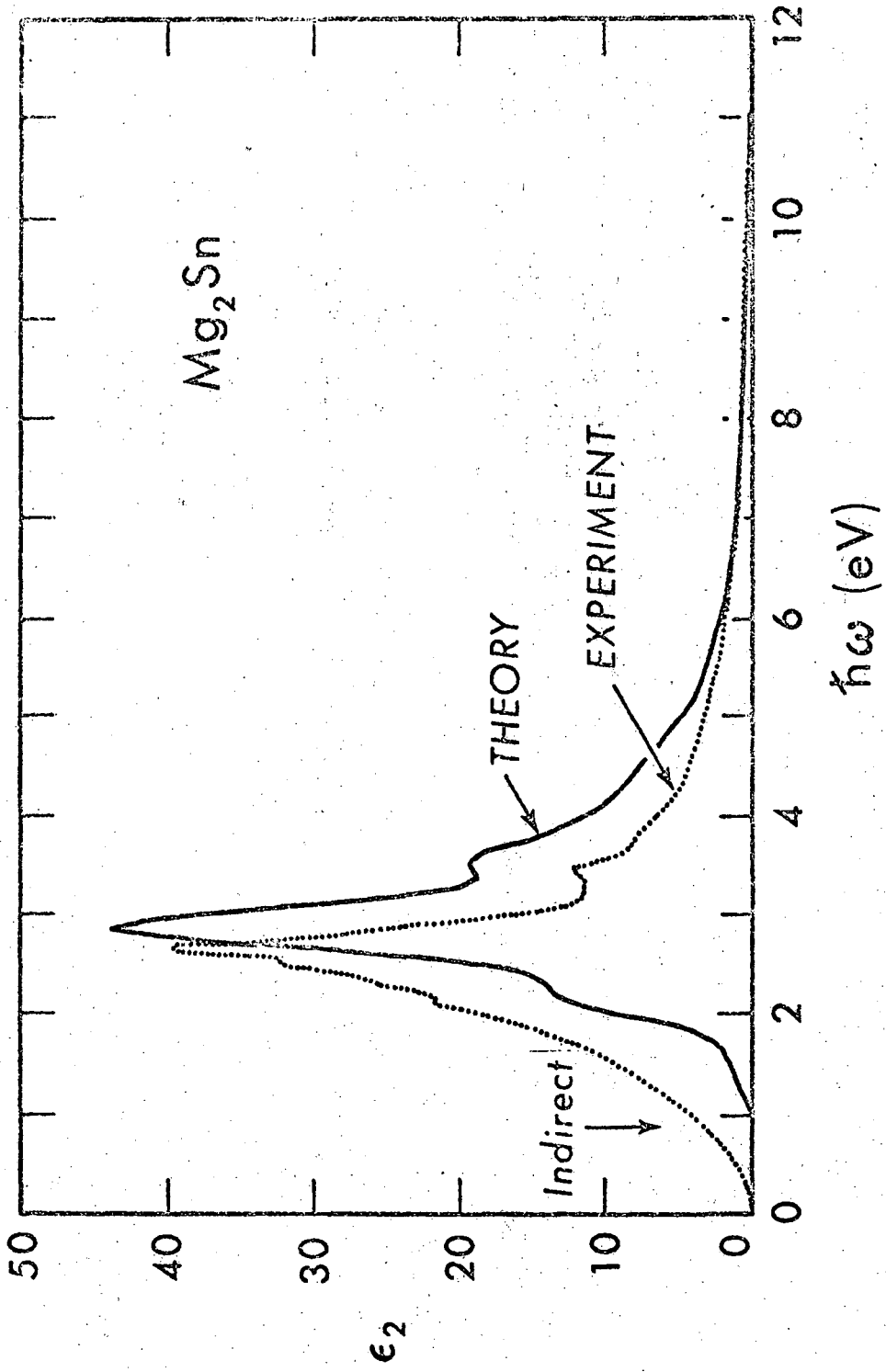


Fig. 6

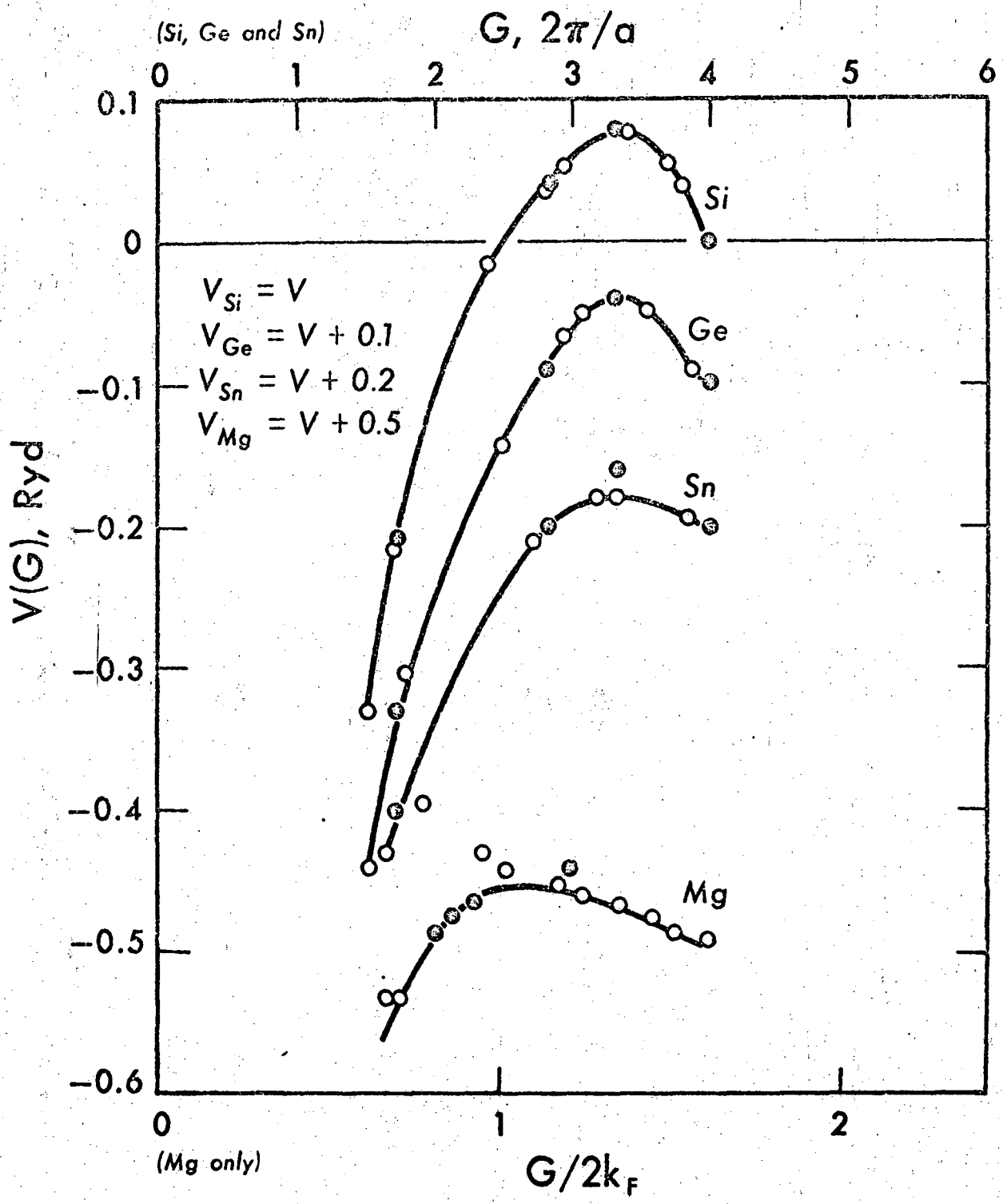


Fig. 7

LEGAL NOTICE

This report was prepared as an account of Government sponsored work. Neither the United States, nor the Commission, nor any person acting on behalf of the Commission:

- A. Makes any warranty or representation, expressed or implied, with respect to the accuracy, completeness, or usefulness of the information contained in this report, or that the use of any information, apparatus, method, or process disclosed in this report may not infringe privately owned rights; or*
- B. Assumes any liabilities with respect to the use of, or for damages resulting from the use of any information, apparatus, method, or process disclosed in this report.*

As used in the above, "person acting on behalf of the Commission" includes any employee or contractor of the Commission, or employee of such contractor, to the extent that such employee or contractor of the Commission, or employee of such contractor prepares, disseminates, or provides access to, any information pursuant to his employment or contract with the Commission, or his employment with such contractor.

TECHNICAL INFORMATION DIVISION
LAWRENCE RADIATION LABORATORY
UNIVERSITY OF CALIFORNIA
BERKELEY, CALIFORNIA 94720